JMEPEG (2012) 21:1214–1219
DOI: 10.1007/s11665-011-0028-8

Facile Design and Fabrication of Two-Way Shape Memory TiNi Springs with Narrow Hysteresis

J.G. Wang

(Submitted December 3, 2010; in revised form June 19, 2011)

In this article, two-way shape memory TiNi springs with narrow hysteresis are fabricated using two-step successive constrained annealing treatments. The as-fabricated springs inherently exhibit two-way shape memory effect (TW-SME) after constrained annealing treatments. The introduction of stable, preferential internal stresses generated by coherent Ti_3Ni_4 phases into the TiNi matrix is indispensable to the TW-SME behavior, which is found to be closely associated with applied strains and the sequence of phase transformations. A simple structural criterion is proposed to ensure the narrow hysteresis. A chart concerning operating temperature points is also plotted as a reference for tracing annealing treatments. The advantages of the springs fabricated by the proposed design consist in its dimensional controllability and long-term cyclability, which are of great importance in the practical application of actuators.

Keywords constrained aging, narrow hysteresis, shape memory alloy, TiNi, two-way shape memory effect

1. Introduction

As functional materials, TiNi shape memory alloys (SMAs) have received extensive attention in industrial and medical fields. Among the functional properties of SMAs, two-way shape memory effect (TW-SME) represents reversible spontaneous shape changes during thermal cycles (Ref 1, 2). The possibility to realize complicated movements using TW-SME makes two-way shape memory actuators very attractive because of the simple design and compact size (Ref 3). However, TW-SME is not an inherent property of SMAs, but it could be developed by proper training methods such as repetitive thermomechanical training routes and constrained aging treatments. To date, a great number of thermomechanical training routes have been studied for the purpose of improving the reversible strain and training procedure (Ref 2-9). The anisotropic microstructure and internal stress field induced by favorable dislocations during Martensite pre-deformation or constrained thermal cycling are responsible for TW-SME. The influencing factors in this case include deformation amount, training temperature, annealing temperature, and thermal cycles. Owing to the shape recovery strain of a straight wire is no more than 1%, a form of spring is thus usually employed to improve the strain, which is also very suitable for better practical investigations. Wang and coworkers (Ref 4-8) have investigated the influence of as-mentioned factors on TW-SME of TiNi-based springs using thermomechanical training routes. However, the obtained reversible strain is unable to be controlled so that the size of spring cannot be designed as expected. On the other hand, new dislocations generated by subsequent thermal cycling will interact with those favorable ones, resulting in a degradation of TW-SME and unstable phase transformation temperatures. Such performances make two-way shape memory springs unsuitable for actuators.

Constrained aging treatments have been considered as a special technique to acquire all-round shape memory effect (AR-SME) (Ref 10). The irregular shape change of a straight wire makes this technique unsatisfactory for obtaining TW-SME, but this technique can produce stable internal stress field, which is generated by the coherent Ti_3Ni_4 precipitates. Takashi et al. (Ref 11) described TW-SME of straight wires aged under a certain tensile stress via measuring strength variation, showing a good TW-SME behavior, but a very small stress-induced reversible strain. The applied stress, Ti_3Ni_4 precipitates, and the induced R-phase were found to have a significant effect on the TW-SME (Ref 12-17). Therefore, it is very interesting to improve the training technique and find a solution to the irregular shape change, thus serving as a useful technique for reversible actuators. Up until now, only a few studies (Ref 16, 17) have paid their attention on these attractive aspects, particularly on the actuator technology.

In the present study, spring is employed to output large displacements and to avoid the irregular shape change. Two-way shape memory springs are fabricated using constrained annealing under a certain external tensile or compressive strain. The purpose of this article is to illustrate the TW-SME behavior in the axial direction of spring and to elucidate the related mechanism. Another purpose is to provide a simple, yet effective technique for designing two-way shape memory springs with narrow hysteresis.

2. Experimental Procedure

A Ni-rich TiNi alloy with a nominal composition of Ti-50.8 at.%Ni was employed in this study. The TiNi wires were prepared by stepwise hot-drawing to a final diameter (d_0) of 0.8 mm, and the semi-finished wires were further straightened by an online straight annealing of 700 °C/60 s. Then, the

J.G. Wang, School of Material Science and Engineering, Tsinghua University, Beijing 100084, China. Contact e-mail: jegonwon@yahoo.com.cn.

straight wire was wound on a spiral mould with a diameter of 6 mm and annealed at 650 °C for 0.5 h, followed by water quenching (WQ). The initial length and pitch of the spring were denoted as L_0 and L_p, respectively. Subsequent to the preliminary shaping, the as-received springs were compressed or elongated to a required length (L_1) and then constrained-annealed at 500 °C for 2 h followed by furnace cooling (FC). The helical spring geometries fabricated and characterized in this study are tabulated in Table 1. The schematic illustration and comparison of thermomechanical training routes and constrained annealing technique were present in Fig. 1.

Phase transformation behaviors of the samples were characterized by DSC (TA Instruments, heating/cooling rate: 10 °C/min). These samples were cut from the springs after the first-step annealing treatment of 650 °C/0.5 h/WQ and the second-step annealing treatment of 500 °C/2 h/FC. Measurements of TW-SME behaviors of the as-prepared springs were preformed on Temperature Displacement Recorder (TDR, a homemade apparatus assembled by a displacement sensor and thermocouple, heating/cooling rate: 2 °C/min). TDR could record the length change of springs in the temperature region ranging from 0 to 100 °C in water bath.

3. Results and Discussion

3.1 Phase Transformation Behaviors

DSC measurements of the phase transformation behaviors of Ti-50.8 at.%Ni alloys (TiNi) after experiencing different annealing treatments are shown in Fig. 2. From Fig. 2, the sample after the first annealing treatment of 650 °C/0.5 h/WQ is observed to exhibit single-stage thermal transformation behavior between Martensite and Austenite (M$\leftrightarrow$A) upon heating/cooling. This indicates the sample is in solid-solution state since the recrystallization temperature of TiNi-based alloys is 600 °C or above (Ref 18). After a subsequent treatment of 500 °C/2 h/FC, the sample undergoes two-stage martensitic transformations upon cooling (A $\rightarrow$ R $\rightarrow$ M) and only one-stage reverse transformation upon heating (M $\rightarrow$ A), typical of aged Ni-rich TiNi alloys. In the cooling process, an intermediate phase of R-phase (R) is induced first from Austenite, implying the precipitation of coherent Ti_3Ni_4 second phases in the matrix (Ref 1, 18). In addition, the starting martensitic transformation temperature (M_S) and other corresponding characteristic temperatures increase rapidly after constrained aging compared to those of the sample in solid-solution state. The DSC results also suggest that the springs in the aged state can fully undergo the complete A $\rightarrow$ R $\rightarrow$ M phase transformations in the temperature region of 0-100 °C. In

Table 1 Geometries of the investigated spring samples

Sample No.	d_0, mm	D_0, mm	L_0, mm	L_p, mm	L_1, mm
1	0.8	7.6	27.5	2.2	32.5
2	0.8	7.6	27.5	2.2	12.0
3(a-e)	0.8	7.6	7.5-9.0	0	16.5-58.5
4					
(a)	0.8	7.6	6.7	0	11.5
(b)	0.8	7.6	8.0	0	14.0
(c)	0.8	7.6	7.5	0	15.3
(d)	0.8	7.6	8.0	0	17.0

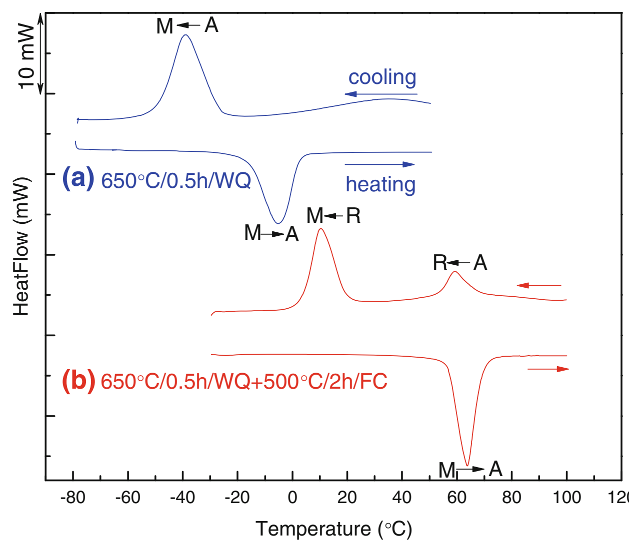

Fig. 2 DSC measurements of the samples with treatments of (a) 650 °C/0.5 h/WQ; (b) 650 °C/0.5 h/WQ + 500 °C/2 h/FC

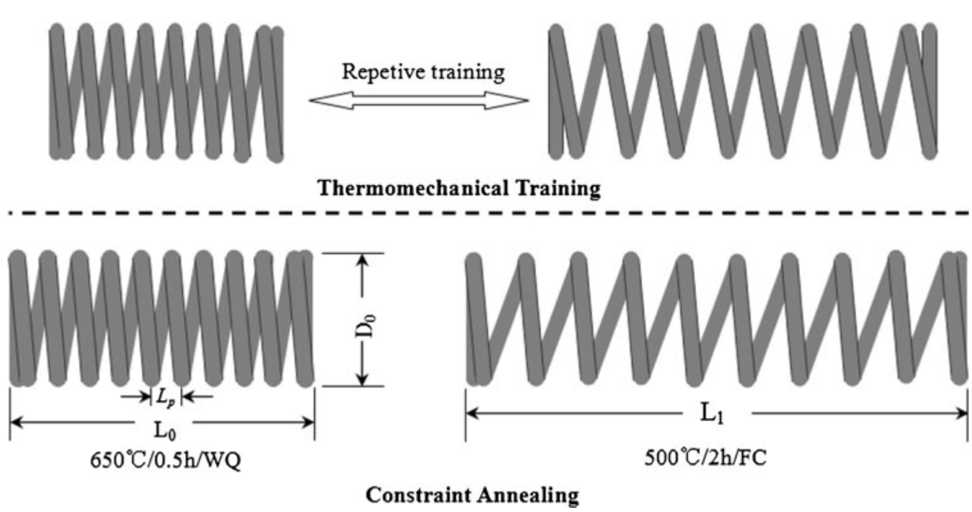

Fig. 1 Schematic illustration and comparison of repetitive thermomechanical training routes and the present constrained-annealing technique

other words, the lengths of the aged springs at 100, 34, and 0 °C could represent the lengths in Austenite state (L_A), R-phase state (L_R), and Martensite state (L_M), respectively.

3.2 Two Way Shape Memory Effect of Springs

Figure 3(a) shows the length change as a function of testing temperature for the spring aged under tensile forces (spring sample No. 1). The initial length of the spring is 27.5 mm, and the deformation amount is 5.0 mm. It is observed that the spring exhibits a complete loop, indicative of perfect TW-SME. The length of the martensitic spring at 0 °C is 17.0 mm. As the testing temperature increases, the spring starts to elongate quickly around 60 °C and finishes to 32.5 mm at 64 °C. By contrast, the curve can be divided into two distinct stages in the cooling process. More specifically, the spring shrinks gradually around 58 °C but keeps a comparatively stable plateau between 44 and 29 °C, and finally shrinks to the martensitic length. This behavior of TW-SME is similar to the phase transformation behavior determined by DSC. Obviously, the elongating process is the result of the reverse transformation (M $\rightarrow$ A), while the shrinking process is associated with two-stage martensitic transformations (A $\rightarrow$ R $\rightarrow$ M). However, the characteristic

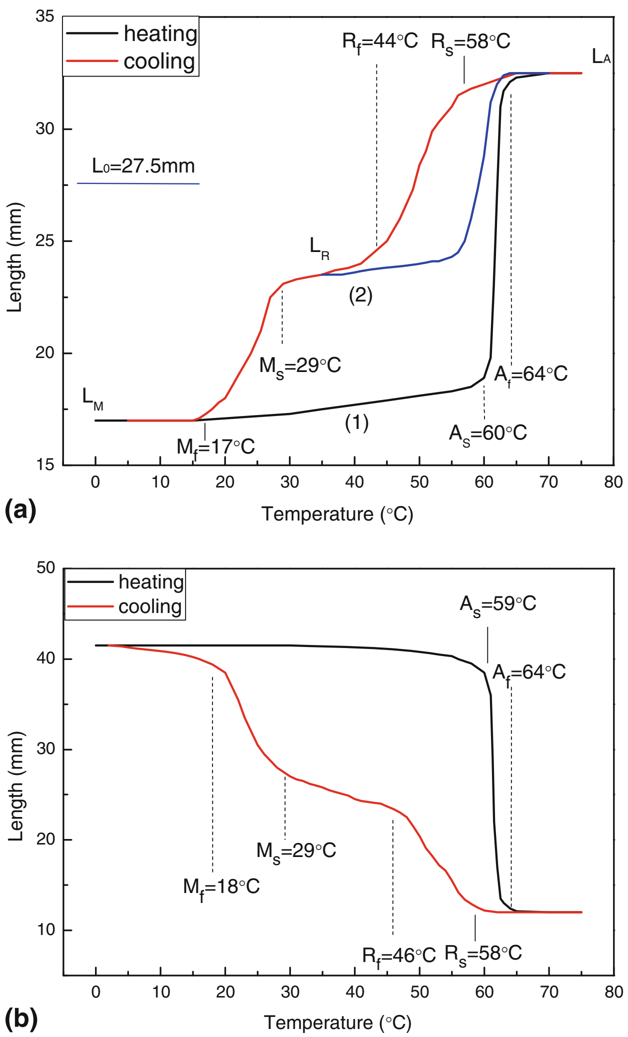

Fig. 3 Two-way shape memory behavior of spring aged under (a) tensile stress (sample No. 1); (b) compressive stress (sample No. 2)

transformation temperatures obtained by TDR are not consistent with those of DSC results. This could be attributed to the different heating/cooling rates used in the measurements (2 °C/min in TDR versus 10 °C/min in DSC). At slower cooling/heating rate, Ms (or other characteristic temperatures) is found to increase more quickly while the transformation temperature interval decreases more rapidly (Ref 19).

Compared with the repetitive thermomechanical training routes, the constrained aging technique does not need a further training process to produce TW-SME, indicating the spring inherently behaves TW-SME. In addition, it is worthy to note that the length of the spring in Austenite state almost equals the pre-applied length. This is of great advantage to the present technique since it can be employed for facile designing and producing an actuator in accurate size. Moreover, as the two-way shape memory strain induced by a straight wire is rather insignificant, the reversible displacement output by the present spring, however, reaches 15.5 mm, which is a remarkable displacement showing a good prospect of practical application in the field of actuators.

Analogously, Fig. 3(b) shows the length change as a function of testing temperature for the spring aged under compressive forces (spring sample No. 2). The pattern of the TW-SME behavior is similar to that of the tensile case as described above, and the only difference is the actuated direction which is just opposite to that of the tensile case. This suggests TW-SME behavior is not only closely related to the sequence of phase transformations but also depends on the type of applied forces. The former determines the step history of TW-SME, while the latter is responsible for the actuated direction upon heating/cooling.

The mechanism of such an inherent property can be explained as follows. It is well known that Ti_3Ni_4 second phases will precipitate in the matrix of Ni-rich TiNi alloys in the intermediate temperature region of 300-500 °C. These Ti_3Ni_4 precipitates are lenticular in shape and coherent to the parent phases, thus creating a coherent stress field (Ref 18, 20). In the case of stress-free aging, an isotropic internal stress may be developed as a result of the randomly distribution of Ti_3Ni_4 precipitates in the matrix. The Martensite (or R-phase) variants in this isotropic internal stress are well self-accommodated to each other upon cooling. However, it is observed by Khalil-Allafi et al. (Ref 21) and Jean and Hu (Ref 22) that Ti_3Ni_4 precipitates align themselves under specific externally applied forces. This specific distribution of Ti_3Ni_4 precipitates creates an anisotropic stress field in the matrix. The direction of the induced stresses tends to be parallel to the tensile forces and be perpendicular to the compressive forces (Ref 11, 16). Consequently, when A $\rightarrow$ R $\rightarrow$ M transformations take place under the anisotropic stress field, variants of R-phase (or Martensite) nucleate and grow preferentially to counteract the anisotropic stress effectively, thus resulting in a macroscopic shape change. Take the case of tensile forces as an example, as schematic illustrated in Fig. 4(a), the anisotropic stress produces a tensile force **F** along the spiral direction of spring which can be decomposed into two component forces of axial force ($\mathbf{F_1}$) and tangential force ($\mathbf{F_2}$). Obviously, $\mathbf{F_2}$ counterbalances each other in a whole spiral circle, i.e., $\mathbf{\Sigma F_2} = 0$. Then, the spring elongates under the control of $\mathbf{F_1}$ upon heating. Upon cooling from the parent phase, the formation of preferential variants gives rise to an expansion to counteract the anisotropic stress, thus leading to the contraction of spring by an opposite force of $\mathbf{-F_1}$. Similar mechanism in the case of compressive forces is also depicted in Fig. 4(b).

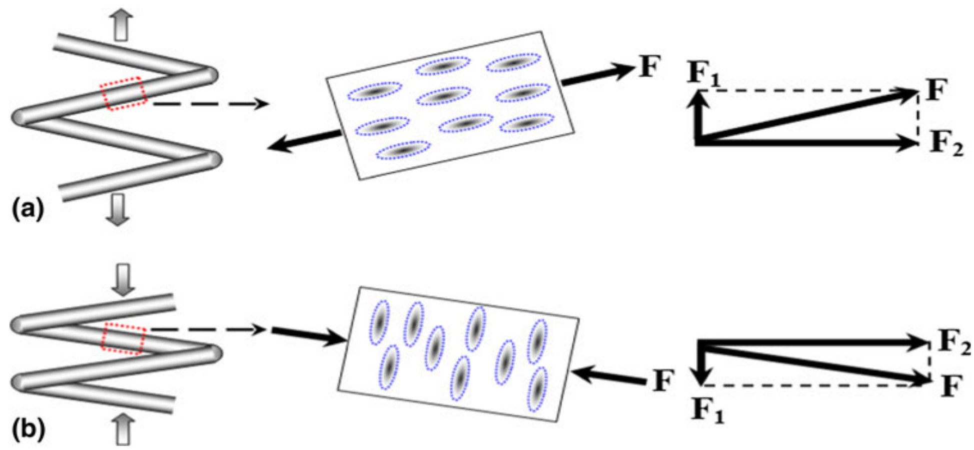

Fig. 4 Schematic illustration of TW-SME mechanism in the case of (a) tensile forces; (b) compressive forces

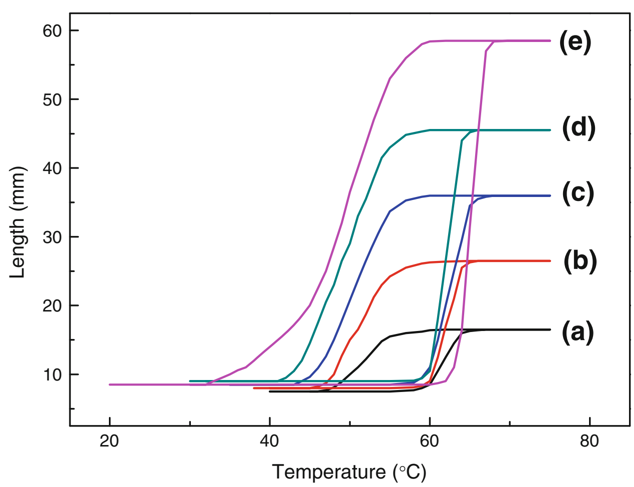

Fig. 5 Effect of tensile deflections on TW-SME with narrow hysteresis (spring sample No. 3(a-e))

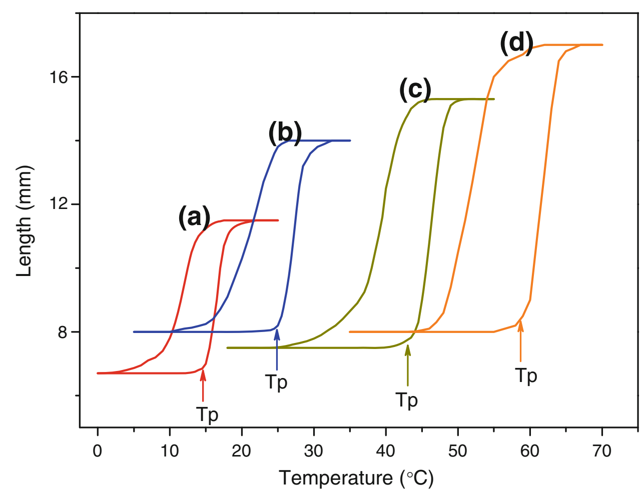

Fig. 6 Representative TW-SME patterns of springs (sample No. 4) with different annealing treatments: (a) 500 °C/0.5 h/WQ; (b) 500 °C/1 h/WQ; (c) 500 °C/6 h/WQ; and (d) 500 °C/2 h/FC. The arrows indicate the operating temperature points

3.3 Two-Way Shape Memory Springs of Narrow Hysteresis

From the cooling branch in Fig. 3(a), it is obvious that the two-stage shrinking process is independent. Therefore, another heating process starting from the intermediate temperature of 34 °C is performed, and the resulting curve (2) is shown in Fig. 3(a). This is a rather narrow hysteresis loop in association with R↔A phase transformations. When one takes a close look at the variation of spring length, the initial length is 27.5 mm, while the length in R-phase state is 23.5 mm, namely, L_A-L_0 is smaller than L_A-L_R. Such a characteristic arouses us to improve spring structure to obtain two-way shape memory springs with narrow hysteresis. Assuming the case of L_A-L_R being greater than L_A-L_0, i.e., when $L_0 \le L_R$, then the spring would not shrink any more when it reaches L_R. Using this criterion, we have prepared a new kind of springs with no pitch ($L_p = 0$) for the first shaping. In the following shaping, the springs were elongated to different lengths with an aim to investigate the effect of tensile deflections on the TW-SME behavior.

Figure 5 presents the TW-SME behaviors of the as-prepared springs (spring sample No. 3), in which complete loops are observed. These loops, as expected, are single-stage processes corresponding to R↔A phase transformations and narrow hysteresis in nature. Although the hysteresis temperature interval increases slightly with increasing the deformation amount, the hysteresis temperature interval herein is still no more than 20 °C, which is far smaller than 50 °C induced by thermomechanical training routes (Ref 4). These results suggest that the structural criterion of $L_0 \le L_R$ satisfies the design of two-way shape memory springs with narrow hysteresis.

Apart from the narrow hysteresis, different operating temperature points (T_ps), because of various practical applications, are required to meet specific requirements. As discussed earlier, T_ps are actually determined by the phase transformation temperatures of R → A which, in turn, can be controlled by annealing treatment in the intermediate temperatures ranging from 300 to 500 °C. It is worth noting that higher annealing temperature results in better shape formability, 500 °C thus being chosen as the annealing temperature for experiments. A series of annealing experiments have been conducted on the second shaping of springs to obtain different T_ps (spring sample No. 4(a-d)). Figure 6 shows representative patterns of two-way shape memory springs with different T_ps. The patterns exhibit

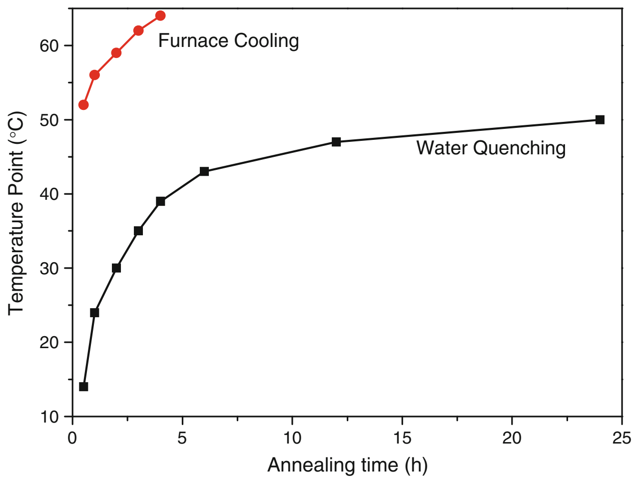

Fig. 7 Effect of annealing time and cooling methods on operating temperature points of springs (annealing temperature: 500 °C)

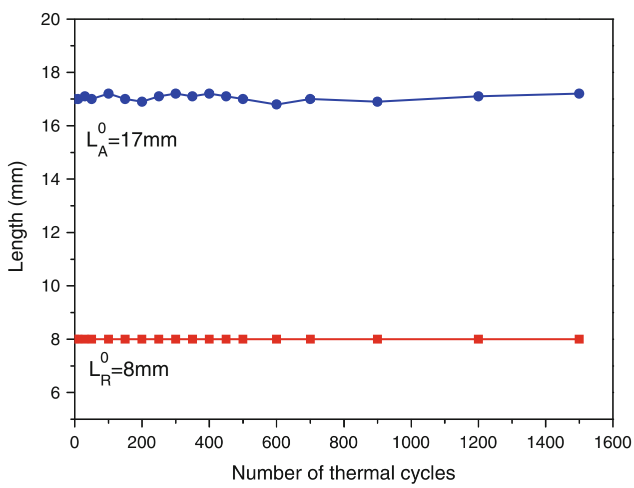

Fig. 8 Size stability of L_A and L_R in novel structural springs as a function of thermal cycles (spring sample No. 4(d))

large similarities with perfect two-way shape memory loops in narrow hysteresis except for the T_ps. The T_ps are controlled by tuning the annealing time and the cooling methods. We believe a chart concerning the relationship between T_ps and the annealing treatments is necessary to be established for reference. Fig. 7 presents the evolution of T_ps as a consequence of annealing time and cooling methods, from which the required temperatures varying from 14 to 65 °C can be traced. This is a wide temperature region available for practical applications.

Another important requirement for actuators is long-term cyclability or size stability. The cycling tests over 1500 cycles of a novel spring (spring sample No. 4(d)) were carried out using TDR in the temperature ranging from 30 to 80 °C. Figure 8 shows the length stability of L_A and L_R as a function of thermal cycles. It can be seen that L_R does not change because of the special structure of spring, while L_A almost stabilizes within the tolerance of 0.2 mm, illustrating the excellent size stability ascribing to the stable internal stress field produced by coherent phases. The outstanding performance enables the spring to maintain a long-term service life for actuators. This is a preliminary investigation into the potential of these springs to function as actuators, but to properly characterize their actuation properties, they must be tested in the presence of applied forces, and this is the focus of ongoing study.

4. Conclusions

Two-step successive constrained annealing treatments provide a simple yet effective technique for developing two-way shape memory springs with narrow hysteresis, particularly suitable for the Ni-rich TiNi-based alloys. The observed TW-SME behavior is closely related to both applied strains and the sequence of phase transformations. R↔A phase transformations are found to be responsible for the narrow hysteresis. A structural criterion of $L_0 \leq L_R$ is proposed as a prerequisite condition for designing a spring with narrow hysteresis. A chart concerning the operating temperature points ranging from 14 to 65 °C is obtained for reference to meet various applications. The springs fabricated by the present technique are characteristic of long-term stability and size controllability, showing a good prospect of practical applications of actuators.

References

1. K. Otsuka and X. Ren, Physical Metallurgy of Ti-Ni-Based Shape Memory Alloys, *Prog. Mater. Sci.*, 2005, **50**, p 511–678
2. H. Scherngell and A.C. Kneissl, Training and Stability of the Intrinsic Two-Way Shape Memory Effect in Ni-Ti Alloys, *Scripta Mater.*, 1998, **39**(2), p 205–212
3. H. Scherngell and A.C. Kneissl, Generation, Development and Degradation of the Intrinsic Two-Way Shape Memory Effect in Different Alloy Systems, *Acta Mater.*, 2002, **50**, p 327–341
4. Y.N. Liu, Y. Liu, and J. Van Humbeeck, Two-Way Shape Memory Effect Developed by Martensite Deformation in NiTi, *Acta Mater.*, 1999, **47**(1), p 199–209
5. Z.G. Wang, X.T. Zu, J.Y. Dai, P. Fu, and X.D. Feng, Effect of Thermomechanical Training Temperature on the Two-Way Shape Memory Effect of TiNi and TiNiCu Shape Memory Alloy Springs, *Mater. Lett.*, 2003, **57**, p 1501–1507
6. Z.G. Wang, X.T. Zu, X.D. Feng, and J.Y. Dai, Effect of Thermomechanical Treatment on the Two-Way Shape Memory Effect of TiNi Alloy Spring, *Mater. Lett.*, 2002, **54**, p 55–61
7. Z.G. Wang, X.T. Zu, X.D. Feng, S. Zhu, J.Y. Dai, L.B. Lin, and L.M. Wang, Study of Two-Way Shape Memory Extension Spring of Narrow Hysteresis TiNiCu Shape Memory Alloys, *Mater. Lett.*, 2002, **56**(3), p 284–288
8. Z.G. Wang, X.T. Zu, P. Fu, J.Y. Dai, S. Zhu, and L.M. Wang, Two-Way Shape Memory Effect of TiNi Alloy Coil Extension Springs, *Mater. Sci. Eng. A*, 2003, **360**, p 126–131
9. E.P. Ryklina, S.D. Prokoshkin, I.Y. Khmelevskaya, and A.A. Shakhmina, One-Way and Two-Way Shape Memory Effect in Thermomechanically Treated TiNi-Based Alloys, *Mater. Sci. Eng. A*, 2008, **481–482**, p 134–137
10. T. Tadaki, K. Otsuka, and K. Shimizu, Shape Memory Alloys, *Ann. Rev. Mater. Sci.*, 1988, **18**, p 25–45
11. F. Takashi, D. Akiyoshi, K. Tomoyuki, and S.T. Toshio, Strength and Martensitic Transformation in Constraint Aged Ti-51 at.%Ni Shape Memory Alloys, *Mater. Trans. JIM*, 1997, **38**(6), p 514–524
12. C. Urbina, S. De la Flor, and F. Ferrando, R-Phase Influence on Different Two-Way Shape Memory Training Methods in NiTi Shape Memory Alloys, *J, Alloys Compd.*, 2010, **490**, p 499–507
13. M.S. Shakeri, J. Khalil-Allafi, V. Abbasi-Chianeh, and A. Ghabchi, The Influence of Ni_4Ti_3 Precipitates Orientation on Two-Way Shape Memory Effect in a Ni-rich NiTi Alloy, *J. Alloys Compd.*, 2009, **485**, p 320–323
14. C.Y. Chang, D. Vokoun, and C.T. Hu, Two-Way Shape Memory Effect of NiTi Alloy Induced by Constraint Aging at Room Temperature, *Metall. Mater. Trans. A*, 2001, **32**, p 1629–1634

15. K. Wada and Y. Liu, On the Mechanism of Two-Way Shape Memory Effect and Stress-Assisted Two-Way Shape Memory Effect in NiTi Shape Memory Alloy, *J. Alloys Compd.*, 2008, **449**, p 125–128
16. J.F. Li, Z.Q. Zheng, X.W. Li, and S.C. Li, Effect of Compressive Stress Aging on the Transformation Strain and Microstructure of Ni-rich TiNi Alloy, *Mater. Sci. Eng. A*, 2009, **523**, p 207–213
17. X.M. Zhang, J. Fernandez, and J.M. Guilemany, Role of External Applied Stress on the Two-Way Shape Memory Effect, *Mater. Sci. Eng. A*, 2006, **438–440**, p 431–435
18. Y.F. Zheng, F. Jiang, L. Li, H. Yang, and Y.N. Liu, Effect of Ageing Treatment on the transformation Behaviour of Ti-50.9 at.%Ni, *Acta Mater.*, 2008, **56**, p 736–745
19. S.H. Chang and S.K. Wu, Effect of Cooling Rate on Transformation Temperature Measurements of $Ti_{50}Ni_{50}$ Alloy by Differential Scanning Calorimetry and Dynamic Mechanical Analysis, *Mater. Char.*, 2008, **59**, p 987–990
20. D. Holec, O. Bojda, and A. Dlouhy, Ni_4Ti_3 Precipitate Structures in Ni-rich NiTi Shape Memory Alloys, *Mater. Sci. Eng. A*, 2008, **481–482**, p 462–466
21. J. Khalil-Allafi, A. Dlouhy, and G. Eggeler, Ni_4Ti_3-Precipitation During Aging of NiTi Shape Memory Alloys and Its Influence on Martensitic Phase Transformations, *Acta Mater.*, 2002, **50**, p 4255–4274
22. R.D. Jean and C.T. Hu, Shape Memory Effect by Constant-Stress Ageing in Ti-505 at.% Ni Alloy, *J. Mater. Sci.*, 2002, **29**(2), p 449–455